Cure Kinetics Modeling and Process Optimization of the ViaLux 81 Epoxy Photodielectric Dry Film (PDDF) Material for Microvia Applications

RAJIV C. DUNNE,[1] SURESH K. SITARAMAN,[1] SHIJIAN LUO,[2] C. P. WONG,[2] WILLIAM E. ESTES,[3] MOOKKAN PERIYASAMY[3]

[1] The George W. Woodruff School of Mechanical Engineering, Georgia Institute of Technology, Atlanta, Georgia 30332

[2] School of Material Science & Engineering, Georgia Institute of Technology, Atlanta, Georgia 30332

[3] DuPont Photopolymers and Electronic Materials, Research Triangle Park, North Carolina 27709

Received 2 August 2000; accepted 9 December 2000

ABSTRACT: The cure kinetics of a photodielectric dry film (PDDF) material called ViaLux 81 has been studied, with the aim of understanding and optimizing its curing schedule for the fabrication of sequentially built-up (SBU) high-density-interconnect printed wiring boards (HDI-PWB). Initial dynamic differential scanning calorimetry (DSC) scans on the material revealed a two-stage curing mechanism due to the long lifetime of the photoinitiator catalyst, which could not be separated at lower heating rates. On the other hand, the heat flow exotherm from isothermal DSC experiments showed a rapid reaction rate at the beginning with only a single peak. Therefore, to capture the complexity of the process, the faster multiple heating rate DSC experiments are used to predict the degree-of-cure (DOC) evolution. Two approaches have been developed based on the dynamic DSC data: (1) a "model-free" approach, which only requires information about the cure-dependence of the activation energy; and (2) a practical scheme to deconvolute the two curing peaks. Excellent agreement is observed for the heating rate experiments, but the methods are inadequate for predicting the DOC evolution under isothermal conditions. Therefore, a modified autocatalytic model with temperature-dependent kinetic parameters has been developed based on the isothermal DSC data. This model predicts the DOC evolution for isothermal curing profiles very well. However, some discrepancy is evident in predicting the DOC evolution for heating rate experiments, due to the underestimation of the activation energy. With appropriate corrections, excellent predictive capability is illustrated for complex cure schedules with combined heating rate and isothermal segments. In addition, a cure process optimization strategy has been suggested, and the fabrication of fine features and microvias is demonstrated. J Appl Polym Sci 84: 691–700, 2002; DOI 10.1002/app.2345

Key words: cure kinetics; Vialux 81 photodieletric dry film; deconvolution; autocatalytic model; microvia fabrication

INTRODUCTION

The widening gap between device and printed wiring board (PWB) interconnect densities, along with the acceleration in semiconductor device feature size reduction, has spurned a high level of interest in high-density interconnect (HDI) sub-

Correspondence to: S. K. Sitaraman (suresh.sitaraman@me.gatech.edu).

Contract grant sponsor: Packaging Research Center; contract grant number: EEC-9402723.

Contract grant sponsor: National Science Foundation; contract grant number: CAREER-DMI-9702285

Journal of Applied Polymer Science, Vol. 84, 691–700 (2002)

strates with sequentially built-up (SBU) microvia technology. One option to create the microvias is to use a photodielectric dry film (PDDF) material, wherein the microvias (interconnect vias) and the conductor lines are mass fabricated by UV irradiation followed by postexposure thermal bake and development in an appropriate solvent. Subsequently, an additive or subtractive electroless and/or electrolytic plating process is used for metallization of the vias and lines. This alternate layering of dielectric and metallization is then sequentially repeated to create a multilayered HDI substrate.[1,2]

Significant warpage and stresses can arise in such multilayered structures during the sequential fabrication process. The magnitude of the warpage and stresses depend on, among other parameters, (1) the degree or the magnitude of the mismatch in the thermomechanical properties, (2) the cure processing conditions, (3) the asymmetric sequencing of the materials layers, and (4) the size and density of interconnects and embedded passives. The thermally induced stresses could result in various failures such as delamination of the layers, film cracking, and microvia cracking; while the thermally induced warpage could lead to misregistration of the fine interconnect features and assembly problems. The most critical step during the fabrication process is the curing of the interlayer polymer dielectric material. As the polymer cures, the thermomechanical properties (modulus, thermal expansion coefficient) develop, and the mismatch in properties between the different materials induces warpage and stresses. It is imperative to investigate the curing kinetics of the polymer in order to develop an appropriate cure process optimization strategy and to understand structure–property relationships, which could thereby lead to a reduction in the process-induced warpage and stresses.

An epoxy-based photodielectric dry film (PDDF) material for HDI applications, called ViaLux 81 is studied in this work. Earlier work by the authors on this material described a complex curing mechanism, with two distinct curing peaks observed in dynamic differential scanning calorimetry (DSC) scan experiments.[3] The first peak was attributed to UV irradiation-induced photolytic decomposition of the cationic photoinitiator to create a superacid (H^+), which promoted ring opening polymerization of the epoxy group. The second peak was due to the thermal decomposition of the photoinitiator to produce additional superacid, which promoted further epoxy polymerization. Based on a study on the effect of exposure dose on curing, a higher exposure dose of 2000 mJ/cm^2 was selected, as this suggested the possibility of reducing the postexposure enhancement bake and final thermal bake time of the dielectric at the expense of a marginal increase in exposure time. Both isothermal and dynamic experiments were conducted, and the activation energy corresponding to the first and second peak was reported to be 129.17 and 124.24 kJ/mol respectively. A cure kinetics model using the multiple heating rate DSC data and a "model-free" approach was also developed. This approach involved the calculation of only a cure-dependent activation energy to predict the evolution of DOC under arbitrary curing conditions. While excellent agreement was obtained for the heating rate experiments, this approach proved to be inadequate for predicting the DOC evolution under isothermal conditions.[3]

Therefore, alternate modeling approaches based on both the isothermal and dynamic DSC data were pursued, and the results are presented in this paper. The isothermal and dynamic DSC experimental data are summarized again to facilitate the explanation of the modeling approaches. The two modeling approaches that have been developed to predict the evolution of DOC are (1) based on dynamic DSC data, using a practical scheme to deconvolute the curing peaks; and (2) based on isothermal DSC data, using a modified autocatalytic model with temperature-dependent kinetic parameters. Additionally, a process optimization strategy is suggested for curing the ViaLux 81 PDDF under isothermal conditions, and the fabrication of microvias and fine features is demonstrated. It should be mentioned that the lack of material composition information makes the kinetic analysis presented here strictly phenomenological in nature.

EXPERIMENTAL

The dynamic heating rate and isothermal DSC measurements were performed in a TA Instruments 2920 MDSC (modulated differential scanning calorimetry) instrument. Due to the presence of some solvents in the material, smaller sample sizes of 5–8 mg were used in hermetically sealed aluminum pans and in a nitrogen purge gas environment. The dynamic heating rate experiments were conducted from room tempera-

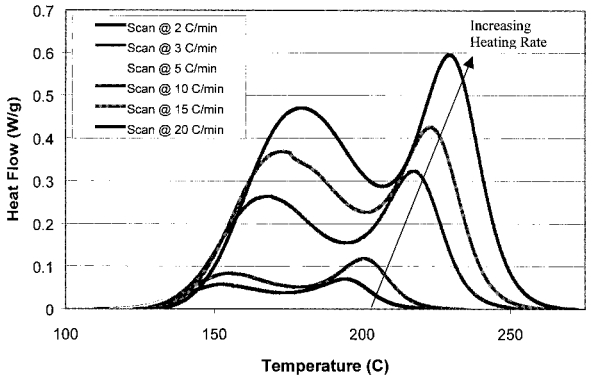

Figure 1 Dynamic DSC data (baseline corrected) at multiple heating rates (exposure = 2000 mJ/cm^2).

ture to 350°C at six different heating rates: 2, 3, 5, 10, 15, and 20°C/min. A subsequent dynamic scan at 10°C/min was done to confirm that the sample had cured completely, and to determine the glass transition temperature, T_g. The isothermal experiments were done from 110 to 175°C in 5°C increments until no further heat flow was observed. A subsequent dynamic scan was done at 10°C/min on each of these samples to determine the residual heat of reaction, if any. The heat flow exotherms from the heating rate experiments are plotted in Figure 1. Figure 2(a) shows the heat flow data for samples cured at different isothermal temperatures. The residual exotherms for the isothermally cured samples are illustrated in Figure 2(b). As can been observed from Figure 2(b), curing is incomplete at all of these temperatures. However, when the cure temperature is increased to 175°C, no residual exotherm is obtained, indicating complete cure of the material. For an additional discussion on these results, please refer to the earlier work by the authors.[3]

CURE KINETICS MODELING

To develop a predictive cure kinetics model for the evolution of degree-of-cure (DOC) with time and temperature under an arbitrary temperature–time curing profile, two approaches have been developed. The basic rate equation associated with the curing kinetics of polymers is first presented, followed by the details of the cure kinetics models based on both dynamic and isothermal DSC experiments.

Basic Theory

The fundamental rate equation that expresses the reaction rate as a function of time or temperature with conversion is

$$\frac{d\alpha}{dt} = k(T)f(\alpha) = Ae^{-E/RT}f(\alpha) \tag{1}$$

where α is the degree-of-cure, f(α) is the reaction model, k is the rate constant, A is the preexponential or frequency factor, E is the activation energy, R is the gas constant, T is the temperature, and t is the time. Under nonisothermal conditions, when the temperature varies with time at a constant heating rate, $\beta = dT/dt$, this equation may be transformed as

$$\frac{d\alpha}{dt} = \frac{d\alpha}{dT}\frac{dT}{dt} = \frac{d\alpha}{dT}\beta = Ae^{-E/RT}f(\alpha) \tag{2}$$

Equation (2) is often expressed in an integral form as

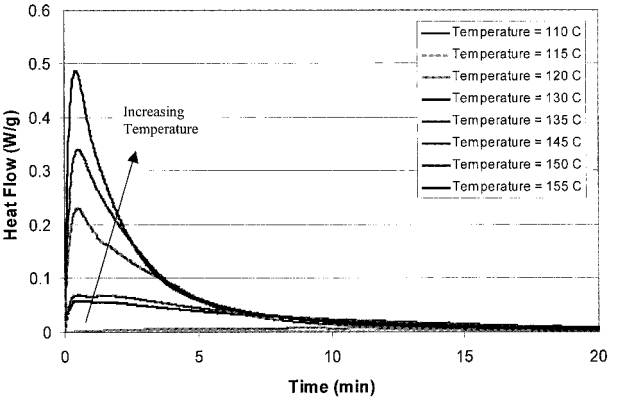

(a)

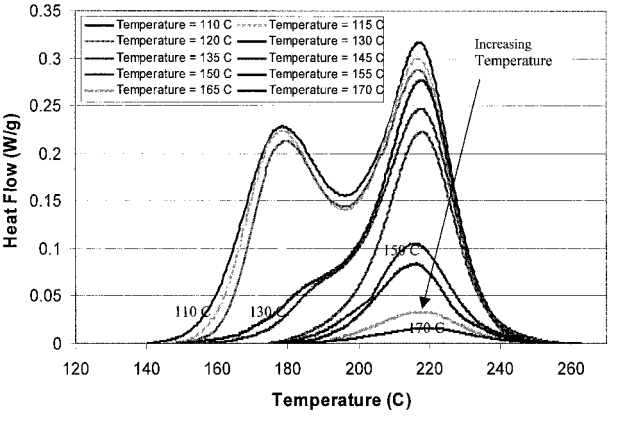

(b)

Figure 2 (a) Isothermal DSC data (baseline corrected) at different temperatures (exposure = 2000 mJ/cm^2). (b) Susequent DSC scan data (baseline corrected) of the isothermally cured samples (exposure = 2000 mJ/cm^2).

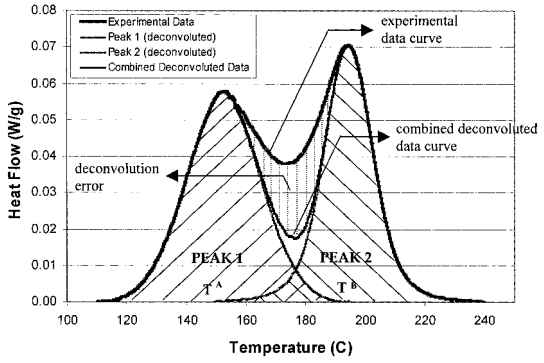

Figure 3 Schematic of the three-segment deconvolution scheme (illustrated with the 2°C/min dynamic DSC data).

$$\int_0^{\alpha} \frac{d\alpha}{f(\alpha)} = g(\alpha) = \frac{A}{\beta}\int_0^{T} e^{-E/RT}dT \qquad (3)$$

For thermosetting systems, the commonly used reaction models are $f(\alpha) = (1-\alpha)^n$ for nth order reactions, and $f(\alpha) = \alpha^m(1-\alpha)^n$ for autocatalytic reactions. Typically, eq. (1) is used for single peak reactions. However, it can be used for multiple peak reactions as well.[4,5]

Cure Kinetics Model from Dynamic Experiments

In an earlier publication by the authors,[3] the evolution of DOC calculated using a model-free approach by Vyazovkin,[6] which only required information about the cure dependence of the activation energy, proved to be inadequate to predict the DOC evolution for isothermal curing conditions.

Therefore, as illustrated in Figure 3, a practical scheme was developed to deconvolute the two peak exotherm in the dynamic DSC data, using the activation energies calculated previously using the Kissinger method.[7] For each heating rate curve, the heat flow data from the beginning until the maxima of the first peak is stored, and reflected to the right about this maxima to create the first-peak area. Similarly, the heat flow data from the maxima of the second peak until the end is stored, and reflected to the left about this maxima to create the second peak area. The data from the two peak areas are then combined by adding the individual peak areas to yield a combined deconvoluted data curve. The difference between this curve and the actual experimental data curve yields the "deconvolution error," which is an indicator of the discrepancy we might expect in predicting the DOC evolution. Each of the peak area curves are normalized to have a DOC from 0 to 1. It should be mentioned that the rationale behind developing this approach was based on the experimental observation that a single peak starting at 165°C was observed on conducting a dynamic DSC scan at 2°C/min on the uncured and unexposed sample, which is consistent with the start of the second peak area reaction.

Next, to find the kinetic model that best describes the nonisothermal experimental DSC data, a useful method suggested by Malek[8] was used. This involves the definition of the function $y(\alpha)$:

$$y(\alpha) = \frac{d\alpha}{dt}e^{(E/RT)} = Af(\alpha) \qquad (4)$$

which is proportional to the $f(\alpha)$ function, and therefore provides information about the type of the reaction model. Since the activation energy is known for both the peaks, $y(\alpha)$ can be obtained for each curve using eq. (4). Shown in Figures 4(a) and 4(b) are the $y(\alpha)$ vs α curves. These curves imply that an autocatalytic model of the form $f(\alpha) = \alpha^m(1-\alpha)^n$ might provide a suitable fit to the data. An intrinsic property of this model is that the maximum occurs at a fixed DOC $\alpha_m = m/(m+n)$. The kinetic parameter ratio $p = m/n$ can be reexpressed in terms of α_m as $p = \alpha_m/(1-\alpha_m)$. To calculate the kinetic parameter n, eq. (1) is rewritten in the form

$$\ln\left[\frac{d\alpha}{dt}e^{(E/RT)}\right] = \ln[y(\alpha)] = \ln A + n\ln[\alpha^p(1-\alpha)] \qquad (5)$$

The kinetic parameter n for each peak area corresponds to the slope of the linear dependence in the $\ln[y(\alpha)]$ vs $\ln(1-\alpha)$ plots [see Fig. 4(c)]. Finally, the frequency factor A is computed using

$$A = \frac{-\beta x_p}{Tf'(\alpha_p)}\exp(x_p) \qquad (6)$$

where $x = E/RT$ is the reduced activation energy, and the subscript p corresponds to the maximum in the experimental DSC curve. The average values for the kinetic parameters calculated for all the heating rate data are tabulated in Table I.

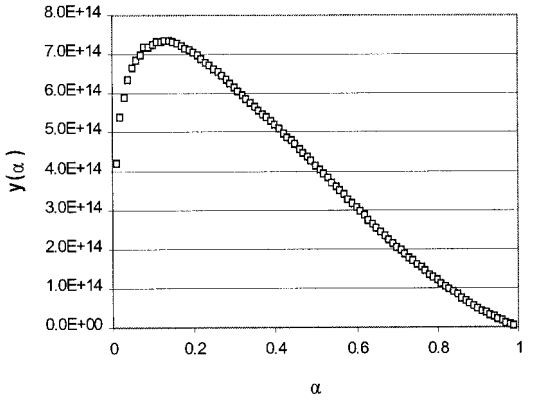

(a)

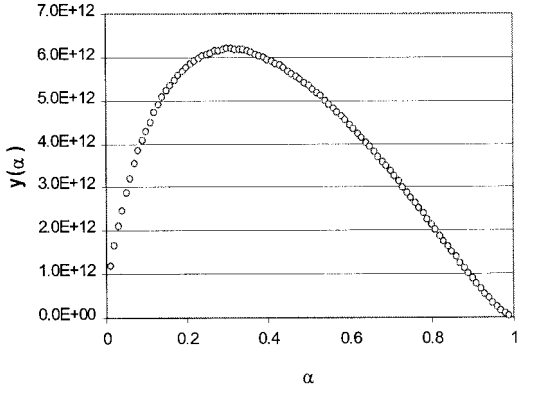

(b)

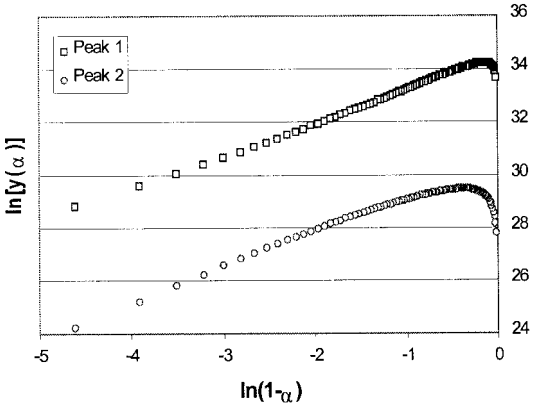

(c)

Figure 4 (a) Peak 1: Variation of $y(\alpha)$ with α (for the 2°C/min dynamic DSC data). (b) Peak 2: Variation of $y(\alpha)$ with α (for the 2°C/min dynamic DSC data). (c) Calculation of the kinetic parameter n (for the 2°C/min dynamic DSC data).

The average deconvolution error was approximately 10%.

To simulate the evolution of DOC with temperature, the fourth-order Runge Kutta method was employed to solve the cure rate equation. The DOC range was split into the following three segments: (1) $0 \leq \alpha \leq \alpha^A$, (2) $\alpha^A < \alpha < \alpha^B$, and (3) $\alpha^B \leq \alpha \leq 1$, where α^A and α^B correspond to the DOC at the onset temperatures T^A and T^B in the actual experimental data curve. The first reaction rate equation was solved in the first segment, followed by a combination of the first and second rate equations in the second segment, and only the second rate equation in the third segment. A comparison of the result obtained using this three-segment deconvolution scheme with experimental DSC results is shown in Figure 5 for $\beta = 2$°C/min. While excellent agreement is evident with the combined deconvoluted data curve, the slight discrepancy with the original experimental data is to be expected due to the deconvolution error. In Figures 6(a) and Figure 6(b), the calculated and experimental results are illustrated for variable heating rate and isothermal cure conditions. These results suggest that this practical approach is good for predicting the DOC evolution in dynamic curing conditions, but is inadequate for curing under isothermal conditions.

Table I Average Values for Ultimate Heat of Cure, Activation Energy, and Kinetic Parameters

	Peak Area 1	Peak Area 2
H_{ult} (J/g)	57.59	46.25
E (kJ/mol)	129.17	124.24
m	0.15	0.57
n	1.38	1.28
$\ln[A]$ (s^{-1})	30.89	26.75

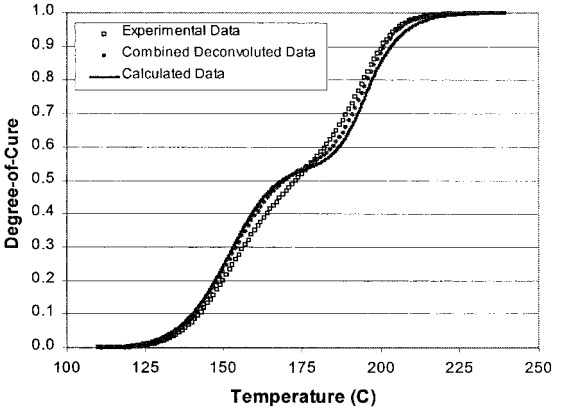

Figure 5 Comparison of the experimental and three-segment deconvolution scheme results (for the 2°C/min dynamic DSC data).

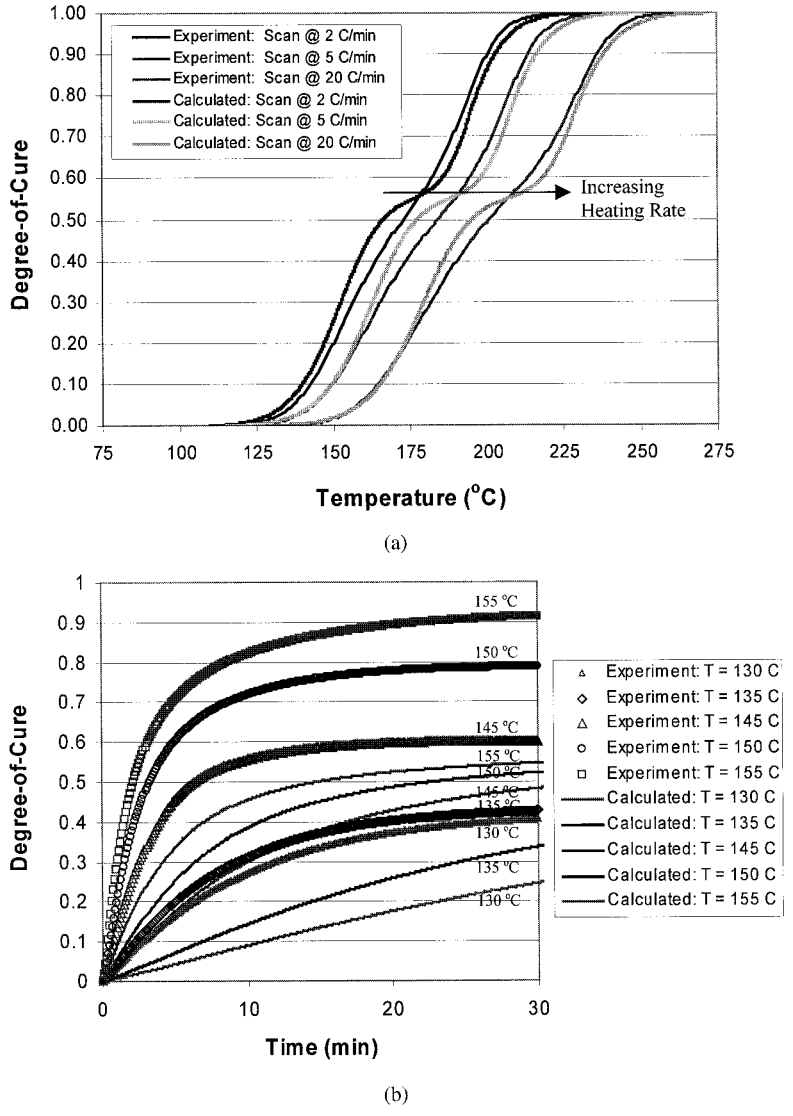

Figure 6 (a) Comparison of the DOC evolution from DSC experiments and the three-segment deconvolution scheme, for multiple heating rates. (b) Comparison of the DOC evolution from DSC experiments and the three-segment deconvolution scheme, for isothermal conditions.

Cure Kinetics Model from Isothermal Experiments

Since the modeling approaches based on the dynamic DSC data were unsuccessful in predicting the DOC evolution under isothermal curing conditions, the isothermal data shown in Figure 2(a) was used to develop a cure kinetics model. Significant heat flow losses could occur at the start in such experiments when the sample is trying to equilibrate at the prescribed isothermal temperature, as well as near the apparent completion, when the reaction rate falls below the sensitivity of the calorimeter. With this knowledge, as well as the fact that very rapid curing rates exist at the beginning at increased cure temperatures, only the isothermal data at 130, 135, 145, 150, and 155°C were considered to develop the model. The plot of cure rate with DOC at these temperatures, as illustrated in Figure 7, clearly shows the increase in cure rate with increasing temperature, as well as the nonconstancy of the activation energy (since the DOC at the maximum cure rate increases with increasing cure temperatures).

A modified autocatalytic model has been developed, which includes the temperature dependence of the maximum DOC achieved at different cure

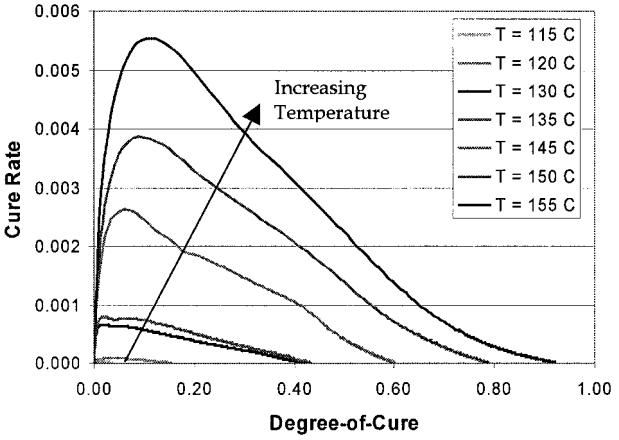

Figure 7 Cure rate vs DOC from isothermal experimental DSC data.

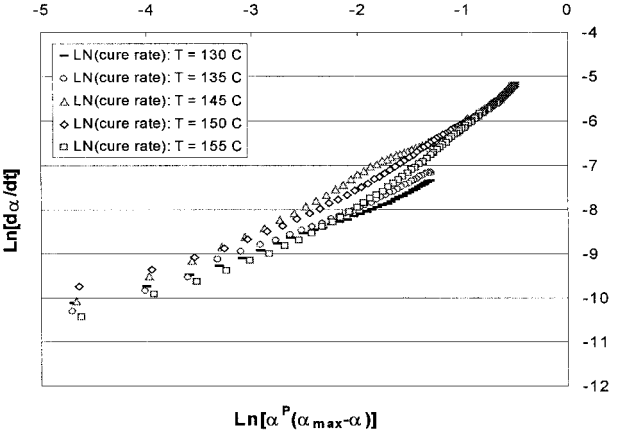

Figure 9 Calculation of the temperature dependence of the kinetic parameter n.

temperatures, as shown in Figure 8. The form of the cure rate equation is shown below[9]:

$$d\alpha/dt = k(T)\alpha^{m(T)}[\alpha_{\max}(T) - \alpha]^{n(T)} \qquad (7)$$

The kinetic parameter n is determined first from the slope of the linear dependence of $\ln[d\alpha/dt]$ vs $\ln[\alpha^p(\alpha_{\max} - \alpha)]$ for each of the temperatures (see Fig. 9). Thereafter, m is calculated as in the previous section, from $p = \alpha_m /(1\text{-}\alpha_m)$, where α_m is the DOC at the maximum cure rate. The rate constant, k, is computed by transposing the reaction model in eq. (7) to the left-hand side. All the computed results for the temperature-dependent kinetic parameters are summarized below:

$$\alpha_{\max}(T) = -0.000005T^3 + 0.0019988T^2 - 0.2453T + 9.4576$$

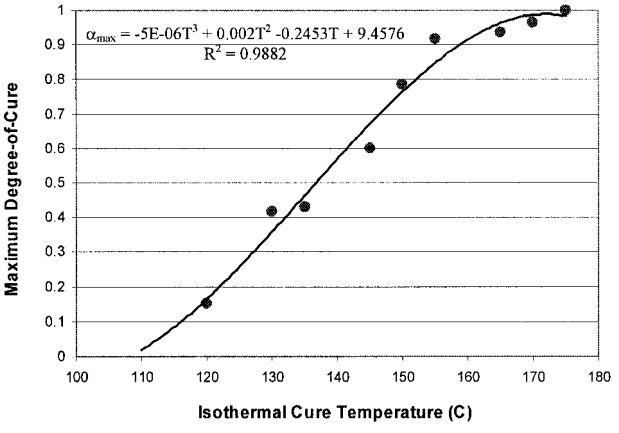

Figure 8 Maximum DOC achieved at various isothermal cure temperatures.

$$m(T) = 0.0041T - 0.4553$$

$$n(T) = 0.0224T - 2.0608$$

$$k(T) = \exp[23.1704 - 11864.2699/T] = A\exp[-98.63/RT] \qquad (8)$$

Solution of the cure rate equation using the fourth-order Runge Kutta method yields the DOC evolution with time. Excellent agreement is evident at the selected isothermal temperatures from Figure 10(a). However, there does exist some deviation in the DOC evolution with temperature for the heating rate experiments [see Fig. 10(b)]. This is primarily due to the underprediction of the activation energy, which may be calculated from the $k(T)$ expression in eq. (8) to be 98.63 kJ/mol. Given the environmental (light and moisture) and solvent effects that affect the DSC thermograms, this discrepancy was manually corrected for by modifying the activation energy in eq. (5) to 124 kJ/mol, which is equivalent to shifting the calculated curves to the right. This modification yields fairly accurate results for the heating rate experiments for temperatures until 175°C, which is the upper temperature limit to achieve full cure of the Vialux 81 material. The discrepancy at higher temperatures cannot be avoided for both isothermal and dynamic heating conditions, since the modified autocatalytic model allows only a single activation energy for the entire process. However, it should be noted that the activation energy selected for correcting the autocatalytic model is consistent with the activation energies computed earlier from the dynamic DSC experiments for

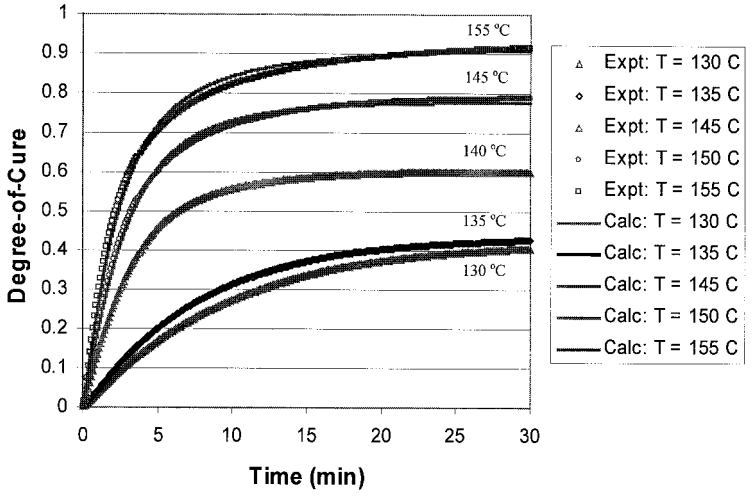

(a)

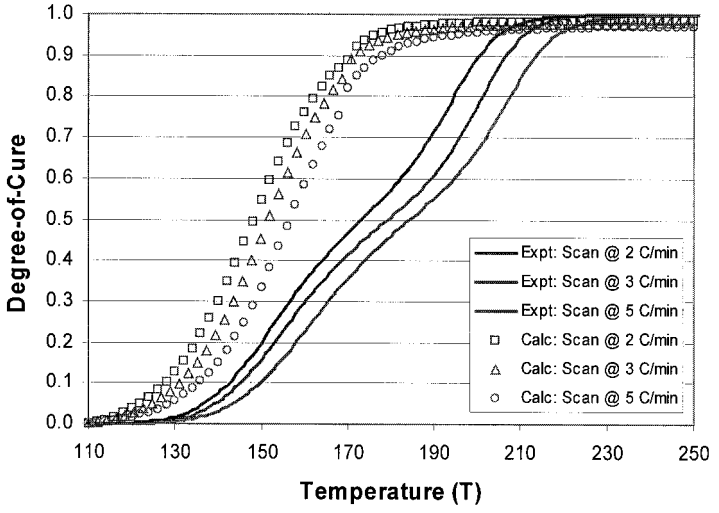

(b)

Figure 10 (a) Comparison of the DOC evolution from DSC experiments and the modified autocatalytic model, for isothermal conditions. (b) Comparison of the DOC evolution from DSC experiments and the modified autocatalytic model, for multiple heating rates.

the two curing peaks, which were 129.17 and 124.24 kJ/mol respectively.[3]

MODEL VALIDATION

To optimize the curing schedule, it is important to validate the predictive capability of the corrected modified cure kinetics model for complicated cure schedules with combined heating rate and isothermal segments. Therefore, a DSC experiment was conducted with an initial heating rate segment of 10°C/min from room temperature to 170°C, followed by an isothermal hold segment at 170°C for 30 min. As shown in Figure 11, fairly good agreement is observed between the calculated and experimental results. This gives us a fair deal of confidence in predicting the cure kinetics for arbitrary cure schedules using the modified autocatalytic model shown in eqs. (7) and (8). Alternatively, one can use a hybrid approach wherein the DOC evolution for heating rate segments is computed using the model-free or deconvolution approach, while the DOC evolution for isothermal hold segments is computed using the modified autocatalytic model.

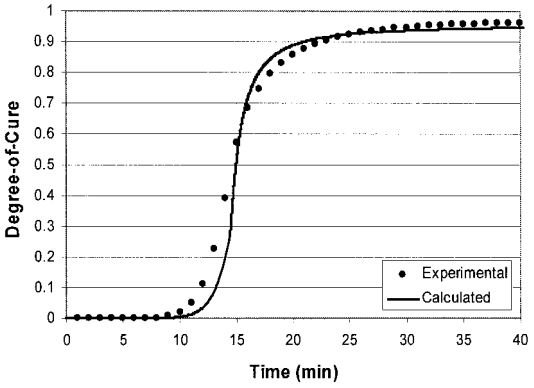

Figure 11 Model variation: 10°C/min heating ramp rate from 25 to 170°C, followed by a 30-min hold at 170°C.

CURE PROCESS OPTIMIZATION STRATEGY

The typical curing process steps for the ViaLux 81 interlayer dielectric material are shown in the schematic in Figure 12. The original manufacturer recommended cure (MRC) cycle conditions consisted of an exposure dose of 1200 mJ/cm^2, a postexposure enhancement bake at 110°C for 1 h, and a final thermal bake at 150°C for 1 h. By increasing the exposure dose to 2000 mJ/cm^2 (selected earlier), the goal was to affect a reduction in the postexposure enhancement bake time and the final thermal bake time, and thereby reduce the cure cycle time. The following cure optimization strategy was adopted here: (1) to reduce the postexposure enhancement bake time at 110°C, a trial-and-error experimentation approach was employed, since the reaction heat flow is very small at this temperature for the cure kinetics model to adequately predict the evolution of DOC, and (2) to optimize the final thermal bake conditions (time and temperature), the modified autocatalytic cure kinetics model was used.

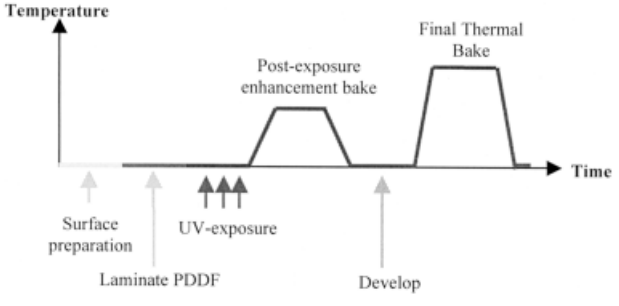

Figure 12 Schematic of process steps for the interlayer dielectric material.

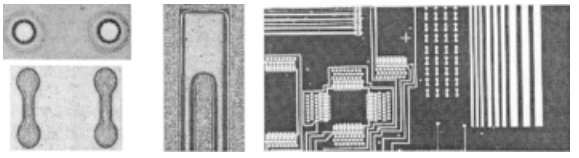

Figure 13 Representative microvias, fine lines and features.

Using this approach, an alternate curing schedule under isothermal cure conditions is suggested. The postexposure enhancement bake time at 110°C is reduced from 60 to 20 minutes, i.e., a 40-min reduction in cure cycle time. Under these conditions, development in γ-butyrolactone (GBL) solvent resulted in the successful definition of fine features and microvias (see Fig. 13). Next, to reduce the final thermal bake time, the cure kinetics model was used to select an isothermal cure temperature of 170°C for 15 min, instead of the original condition of 150°C for 1 h. This implies a 45-min reduction in the cure cycle time, and results in a maximum DOC of 94%. It should be emphasized that while a high DOC implies better electrical and thermomechanical properties, it might lead to a significant reduction in plated copper adhesion with the polymer. Therefore, additional experiments were done to assess the adhesion peel strength (under constant swell/etch, electroless and electroplating conditions) for cure temperatures in the range from 150 to 185°C. In all the cases, the peel strength was greater than 5 lbs/in. Another concern was the increase in residual stress that would result due to the increase in the cure temperature. Interestingly, the residual stress, measured using the Flexus Thin Film Stress Measurement Apparatus (TFSMA) Model 2-300, only varied between 15 and 17 MPa for cure temperatures in the range from 150 to 185°C.

CONCLUSIONS

DSC experiments on the ViaLux 81 PDDF UV exposed to 2000 mJ/cm^2 reveal a high degree of complexity in the curing mechanism. Two modeling approaches are presented in this work to predict the evolution of DOC: (1) based on dynamic DSC data, using a practical scheme to deconvolute the two curing peaks, and (2) based on isothermal DSC data, using a modified autocatalytic model with temperature-dependent kinetic pa-

rameters. The predictive capability of the cure kinetics model based on dynamic DSC data was found inadequate for arbitrary heating conditions. However, with due consideration to environmental and solvent effects and to the unavailability of material composition information, the isothermal data based model produced reasonable results even with complex curing schedules having combined heating rate and isothermal segments. Subsequently, the cure cycle time was reduced by over an hour through a suitably designed cure process optimization strategy for isothermal curing conditions. Furthermore, using the suggested cure schedule, the fabrication of microvias and fine features within the ViaLux 81 material has also been successfully demonstrated.

Future work will include a thorough investigation into the feasibility of other cure processing histories [thermal convection ovens, hot plate curing, and rapid thermal curing (RTC) in continuous belt furnaces]. Besides, the cure kinetics analysis will be used in conjunction with the ongoing thermomechanical characterization of ViaLux 81 PDDF to develop cure-dependent phenomenological models for the viscoelastic stress relaxation modulus and the coefficient of thermal expansion, inclusive of polymerization-induced shrinkage effects.

The authors would like to acknowledge the support from the Packaging Research Center (Contract No.: EEC-9402723) and the National Science Foundation (CAREER-DMI-9702285).

REFERENCES

1. Coombs, C. F. Printed Circuits Handbook; McGraw-Hill: New York, 1988.
2. Dunne, R. C.; Sitaraman, S. K. Proc Electron Compon Technol Conf, 48th, IEEE, Piscataway, NJ, 1998, 351.
3. Dunne, R. C.; Sitaraman, S. K.; Luo, S.; Wong, C. P.; Estes, W. E.; Gonzalez, C. G.; Coburn, J. C.; Periyasamy, M. J Appl Polym Sci 2000, 78(2), 430.
4. Duswalt, A. A. Thermochim Acta 1974, 8, 57.
5. Barton, J. M. Adv Polym Sci 1985, 72, 111–154
6. Vyazovkin, S. Int J Chem Kinet 1995, 28, 95.
7. Montserrat, S.; Flaque, C.; Pages, P.; Malek, J Appl Polym Sci 1995, 56, 1413.
8. Malek, J. Thermochim Acta 1992, 200, 257.
9. Kenny, J. M.; Trivisano, A. Polym Eng Sci 1991, 31, 19, 1426.